

# Comparing Online Circular Contrast Perimetry and the Esterman Visual Field Test in Glaucoma for Driving-relevant Vision

Alexandra Klejn, MBBS, MPH,\* Angela Gong, BBiomedSc,† and Simon E. Skalicky, PhD†

**Précis:** Online binocular perimetry showed moderate to strong agreement with Esterman visual field testing in glaucoma patients and controls, with high correlation coefficients and predictive capability. This tool may offer a viable, accessible alternative to machine perimeters for driving licence assessment.

**Purpose:** To assess the feasibility of an online computer-based binocular driving perimetry assessment (OBDP) based on online circular contrast perimetry, and agreement with binocular static Esterman visual field testing (EVFT).

**Methods:** A prospective comparative cohort study was conducted on patients with or without open angle glaucoma, recruited from a single-site glaucoma subspecialty practice. Eligible subjects underwent 2 visual field tests using OBDP and this was compared with the results of a single EVFT.

**Results:** Eighty patients were enrolled in the study, with a mean age of 69 years ( $\pm 13.4$  SD). Of these, 49% were female, 18 were healthy controls, while 20, 18 and 24 had mild, moderate and severe glaucoma, respectively. Pearson and intraclass correlation between the 2 perimetry methods for percentage of points not seen (PNS) was 0.85 and 0.86 (95% CI: 0.78–0.9), respectively, for the overall binocular visual field. When the binocular field was subdivided into 8 sectors, intraclass coefficients (ICCs) ranged from 0.76 to 0.93 for each sector. Bland-Altman analysis revealed a difference of 1.24% (95% CI: -16.93% to 19.30%) between the 2 methods for the overall field, ranging from 0.04% to 4.17% for each sector. On the basis of the Austroads fitness to drive guidelines, OBDP demonstrated a sensitivity of 96.97% and specificity of 78.57% when compared with the EVFT. ICCs evaluating the repeatability of OBDP testing for the percentage of PNS were excellent overall (0.97) and ranged from moderate to excellent for each of the 8 sectors (0.67–0.98).

**Conclusion:** OBDP showed strong agreement with EVFT. As an online application that easily runs on any computer, it could expand the scope of binocular perimetry screening for licence assessment. With modifications, integration into modern clinical licensing procedures could be considered.

**Key Words:** glaucoma, perimetry, visual field, esterman, online

(*J Glaucoma* 2025;34:1024–1035)

Received for publication October 11, 2024; accepted September 7, 2025. From the \*Launceston Eye Institute, South Launceston, TAS; and †Department of Ophthalmology Surgery, University of Melbourne, VIC, Australia.

Primary author A.K. and secondary author A.G. have no proprietary or commercial interest in any materials discussed in this article. S.S. is a director of Eyeonic Pty Ltd, which owns patent WO2021051162A1 regarding online circular contrast perimetry.

Disclosure: S.S. is a director of Eyeonic Pty Ltd, which owns patent WO2021051162A1 regarding online circular contrast perimetry. The remaining authors declare no conflict of interest.

Reprints: Simon E. Skalicky, PhD, Franzco, A/Prof Simon Skalicky, 2/232 Victoria Pde East Melbourne, Victoria 3000, Australia (e-mail: seskalicky@gmail.com).

Copyright © 2025 Wolters Kluwer Health, Inc. All rights reserved.  
DOI: 10.1097/IJG.0000000000002634

Perimetry remains an important tool for diagnosing and monitoring glaucoma, as well as the assessment of central and peripheral visual thresholds to meet regional driving standards. Several new devices have been developed to make perimetry more portable, including applications on tablets and laptops, virtual reality headsets, and web-based applications, to allow patients to access visual field testing outside of clinics.<sup>1–8</sup> Portable perimetry offers the advantage of fewer in-person clinic visits, lower health care costs, increased access to care, improved user experience, and opportunities for more frequent monitoring between clinic visits.<sup>9,10</sup>

While specific requirements vary between jurisdictions, binocular perimetry is a widely accepted modality for assessing visual fitness to drive in many countries.<sup>11,12,13</sup> It is most commonly performed as an automated, static, suprathreshold test using the Humphrey Field Analyzer (HFA) using stimuli of fixed luminance.<sup>14</sup> This is known as a binocular Esterman visual field test (EVFT).

Online Circular Contrast Perimetry (OCCP), recently developed by Eyeonic Pty Ltd, is a validated perimetry application that enables visual field testing from any personal computer (PC) or tablet device, with no additional hardware requirements. Initially, an age-standardized normative data set was established for 24-2 and 10-2 OCCP testing, through the acquisition of adequately consistent test results from normal participant cohorts.<sup>8,15</sup> In 2 separate studies, patients demonstrated a preference for using OCCP over SAP.<sup>16,17</sup> OCCP has been shown to have similar perimetric outcomes and ability in distinguishing glaucoma patients from controls for SAP,<sup>17,18</sup> although the relationship between OCCP and full threshold perimetry has not been established as for SAP using the SITA strategies.<sup>19</sup> The repeatability of OCCP was evaluated in a cohort of 36 patients monitored 6 weekly over 18 weeks,<sup>20</sup> with good repeatability and reliability with similar performance indices to SAP in the short-term and lower performance in the intermediate term. OCCP is now registered for clinical use in several countries, including Australia (TGA Approved), New Zealand, the UK, the USA (FDA registered), and several African and Asian countries.

To streamline driving licensing assessment and complement the existing 10-2, 24-2, and 30-2 OCCP tests, a binocular suprathreshold perimetry test has been developed with parameters tailored to drive-thru requirements. Like other OCCP protocols, the online binocular driving perimetry (OBDP) test has been specifically designed to provide perimetry on any computer screen through a web application; unlike the other protocols but like EVFT, the OBDP uses suprathreshold testing. In the current study, OBDP was compared with conventional EVFT to assess its

feasibility, accuracy, and suitability for drive-thru assessment, in a mixed cohort of glaucoma patients and normal controls.

## METHODS

A prospective cohort study was conducted on patients with open angle glaucoma and healthy controls who were recruited from a single-site glaucoma subspecialty practice in Melbourne, Victoria, Australia in 2023. Eligible subjects were invited to participate in the study after providing informed consent. Ethical approval was provided by the Royal Australian College of Ophthalmology Human Research and Ethics Committee. The study adhered to the tenets of the Declaration of Helsinki.

Eligibility required participants to be over 18 years of age, able to provide informed, written consent, and able to read and understand the English instructions. Best-corrected visual acuity at baseline had to be  $< 0.7 \text{ logMAR}$ .

Patients with any other significant ocular condition that may influence visual function, such as corneal opacity or scarring, visually-significant cataract according to the LOCS III grading system (Lens Opacities Classification System),<sup>21</sup> non-glaucomatous optic neuropathy or other neuro-ophthalmic condition, significant cognitive impairment, retinal or macular pathology, or previous ocular laser or surgery in the last 12 months were excluded from the study.

## Assessment of Clinical Parameters

The study's principal investigator (consultant ophthalmologist and author SS) conducted a thorough ophthalmic assessment of all the participants to identify any factors that might warrant their exclusion from the study. Baseline data collected included the following clinical parameters: refractive correction for distance, best-corrected visual acuity, Cirrus OCT of the optic nerve head and macula (Carl Zeiss Meditec Inc., Dublin, CA), central corneal thickness (CCT) using the PachMate handheld pachymeter and intraocular

pressure (IOP) using the Goldmann applanation tonometer (Haag-Streit International, Bern, Switzerland).

Control subjects were defined as having normal retinal nerve fiber layer (RNFL) thickness, optic nerve head (ONH) appearance, and standard automated perimetry (SAP) results, without additional ocular pathologies. Glaucoma subjects were defined as those with distinctive disc and VF changes. Eyes were defined as glaucomatous according to criteria outlined by the American Academy of Ophthalmology, with severity of disease was classified using the better-eye visual field mean deviation (MD) as follows:  $\geq -6 \text{ dB}$  (mild), between  $-6 \text{ dB}$  and  $-12 \text{ dB}$  (moderate), and  $\leq -12 \text{ dB}$  (severe), according to Hodapp-Parrish-Anderson Criteria.<sup>22,23</sup>

## Visual Field Testing

Visual field testing for EVFT was carried out binocularly using the Humphrey Field Analyzer (HFA)<sup>23</sup> Esterman strategy, with suprathreshold testing set at 10 decibels. The test was performed in a static rather than roving fashion to match the OBDP, which is also a static test.

The OBDP and EVFT were compared with the HFA 24-2 test using the SITA Standard strategy. The most recent HFA 24-2 tests from the left and right eyes were obtained for each participant, where available. As the 24-2 program does not support binocular testing, results from both eyes were merged to create a binocular integrated visual field (IVF) following a method described by Ishibashi et al,<sup>24</sup> in which the higher sensitivity value at each overlapping point was taken as the sensitivity threshold for that location, approximating binocular performance. For participants with only testing results from one eye available (19 out of 80), the monocular field was used without integration. As the EVFT uses 10 dB as the cutoff for suprathreshold testing, the same threshold was applied to the IVF: sensitivities  $< 10 \text{ dB}$  were considered "not seen," and those  $\geq 10 \text{ dB}$  were classified as "seen."

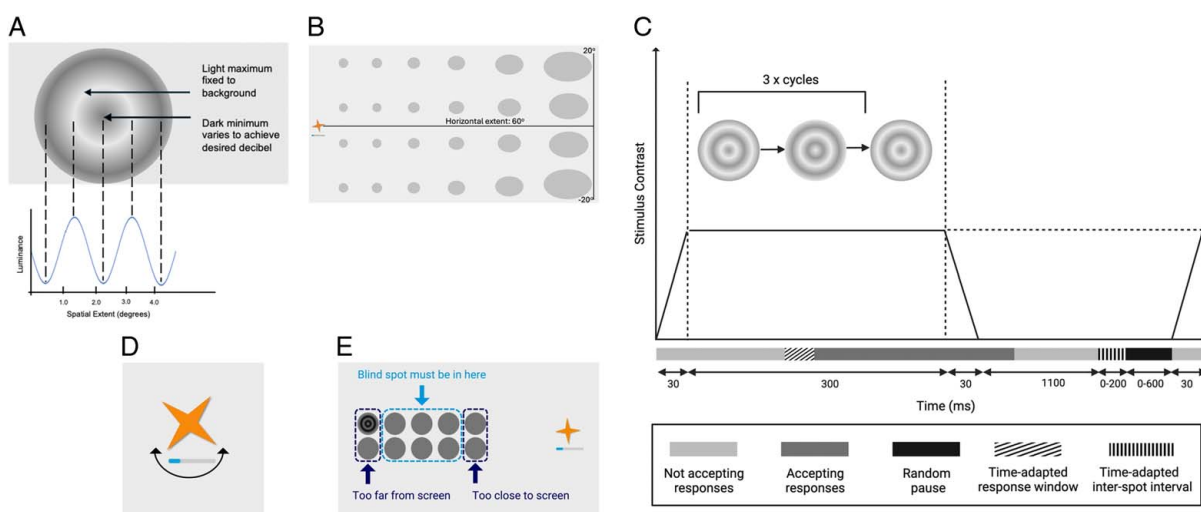


**FIGURE 1.** Online circular contrast perimetry test settings. (A) Flickering test target. (B) Map of loci position and size used in the online binocular driving perimetry test (right side). To test the left side, the fixation target later moves to the far right of the screen. (C) Sequence of target presentation: targets appear for 3 counterphase flicker cycles lasting 360 ms, contrast is graded at the start/end of target presentation. ms indicates millisecond. Figure adapted from Alawa et al.<sup>5</sup> (D) Fixation target: spinning golden star. (E) Blind spot localization optimizes the user's viewing distance. B and E. The dark gray homogenous circles are a diagrammatic representation of where test targets may appear and are not present during the live test. Figure 1 can be viewed in color online at [www.glaucjournal.com](http://www.glaucjournal.com).

## OCCP Assessment

OCCP (Eyeonic, Melbourne, Australia) offers web-based perimetry accessible without additional hardware on any electronic device and has been thoroughly described in previous papers.<sup>8,15-17,20</sup> Its targets share similarities with Pulsar Perimetry (Haag-Streit International); however, Pulsar target is larger and becomes more faint towards the target's periphery; in comparison OCCP targets maintain consistent contrast across their spatial extent (ie, the dark rings at the periphery are as dark as the dark rings in the center, and the same is true of the light rings in the periphery v the center of the target), despite a slight reduction at the target's peripheral edges to minimize light scatter and unintended stimulation of ganglion cells (Fig. 1A).<sup>25,26</sup> The placement of test loci on the monitor, relative to fixation, is adjusted using simple trigonometry to correct for flat plane viewing, as is the size and spread of the loci (Fig. 1B).

Each target undergoes a flicker lasting 60 ms across 3 on/off cycles, totaling 360 ms. The window request Animation Frame object with a timestamp callback in the JavaScript code allows for precision of timing measurements for loci presentations, despite potential inconsistencies in screen refresh rate. Similar to traditional frequency doubling perimetry (FDP),<sup>27</sup> targets exhibit sinusoidal contrast with a spatial frequency of 0.5 cycles/degree but temporal counter phase flickering is slower than FDT at 9 hertz (Hz).<sup>28,29</sup> The contrast is further ramped up and down linearly over 50 ms at the beginning and end of each target presentation to prevent temporal transients and saccades (Fig. 1C).<sup>30,31</sup> In contrast to traditional FDP, where target bands vary around a mean background luminance, OCCP's light rings adopt the background screen color (light gray), while the dark ring intensity varies to achieve desired target contrast levels, similar to using a luminance pedestal flicker for stimulus decrements, as described by Anderson and Vingrys.<sup>32</sup> As the gamma function can vary between screens, and it is impossible, therefore, to predict which greyscale color is the true mean of the dark ring minimum and light ring maximum, this approach aims to reduce the number of greyscale colors present to increase the consistency of display parameters.

To account for varying screen sizes, the application measures the screen size and advises the user at what distance to sit from the monitor, to ensure consistency of viewing angle. It also recalibrates the position and size of the spots accordingly.

Relative luminance is calculated for each 256-bit greyscale level following the Web Content Accessibility Guidelines standards for relative luminance calculation, with output from the test ranging from pure white (255, 255, 255) indicating 100% relative luminance, to black (0, 0, 0) signifying 0%.<sup>33</sup> The contrast of targets was then determined using the Michelson formula, comparing the peaks and troughs of the target rings<sup>34</sup>:

$$\text{Contrast} = (RL1 - RL2)/(RL1 + RL2)$$

Where RL1 represents the light band maximum and RL2 the dark band minimum relative luminance.

Background screen luminance was set to produce an output of 224 candela per square meter (cd/m<sup>2</sup>). Contrast was then converted to decibels using the same approach used in FDP.<sup>28</sup>

$$\text{Relative decibel (dB)} = -20 \log (\text{contrast sensitivity})$$

Utilizing the above formulae the dynamic range for target intensity of OCCP is from 0 to 38 dB. While calculated in a different manner to SAP,<sup>4</sup> this range adequately assesses human threshold estimates across the visual field.

Throughout the test, users are instructed to maintain their gaze on a continuously spinning fixation point (golden star) and click the mouse or press space bar when they see a target in their peripheral vision (Fig. 1D). A distinct sound is generated upon the user's click and varied based on whether the click occurred within the accepted response window or outside—an affirmative, comforting sound is generated each time the user clicks at the correct time (Fig. 1C). Clicks occurring outside the response window produced a negative sound similar to the noise generated when an error occurs during a computer game, indicating a false positive (FP) response.

To account for interuser response rate variability, the interstimulus interval is measured and adjusted based on the user's previous responses (ie, lengthened for individuals with slower response rates and shortened for those with quicker response rates), to ensure that the test proceeded at a suitable pace for each individual.<sup>35</sup>

Measurement of FPs, that is, clicking when no target is present, is particularly important for a driving assessment. This is because poorly seeing patients can be incentivised to click more than what they see, in an effort to pass an otherwise failing test. FPs will pick up such "trigger happy" patients and can be used to disqualify an otherwise successful test result. OCCP has a catch trial functionality for accurate measurement of FPs, occurring when patients click outside the window of accepted responsiveness of a prior target. In addition, the catch trial functionality of OCCP is enhanced by the interstimulus interval substantially expanding if any FPs occur, and an in-built random delay that is introduced between stimuli to prevent rhythmic responses.

OCCP has several carefully chosen design features included specifically to account for variations in screen output and background brightness. This includes the target type, size, flicker rate, and background.<sup>36,37</sup> In addition, the application contains internal calibration mechanisms based on early responses that are carefully measured to determine the normal expected threshold. When utilized in the patient's home environment the application will request that the user increase screen brightness to at least 75%; all of these features combined aim to provide consistency despite such variations.

## The Online Binocular Driving Protocol

Using the testing parameters of OCCP, the OBDP protocol evaluates 48 loci spanning 120×40 degrees of peripheral vision by presenting users with circular flicking targets characterized by concentric alternating dark and light rings, each measuring 3 degrees of visual angle with 10 degrees of spatial separation (Fig. 1B).

The EVFT uses 10 dB as the standard threshold for testing using SAP. The OBDP, based on OCCP, similarly uses suprathreshold targets set at 10 dB for central loci. While the physiological parameters and formulae for the derivation of SAP and OCCP are different, the OCCP was crafted and validated against SAP to achieve a similarity in

## Visual Field Result

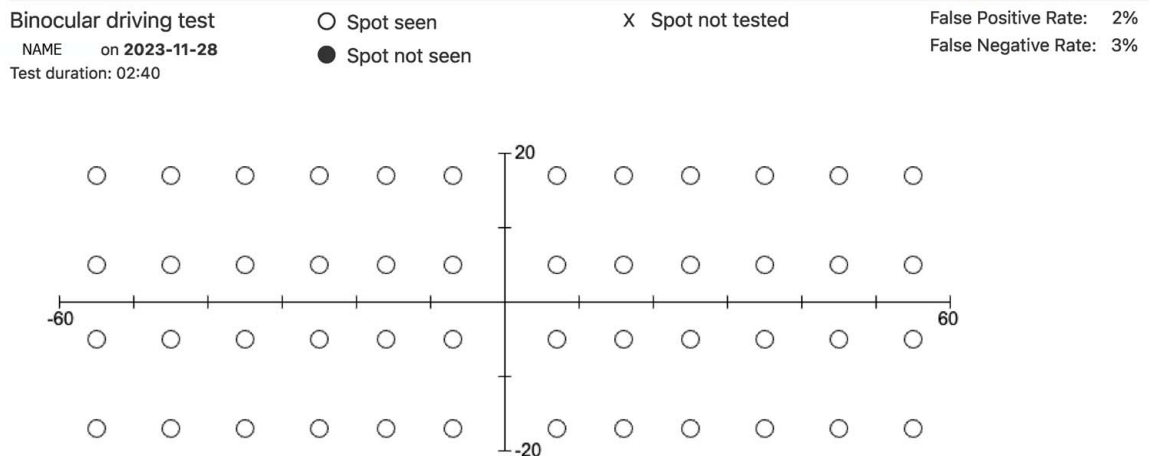


**FIGURE 2.** Online binocular driving test sample printout, 40 degrees vertically versus 120 degrees horizontal suprathreshold test. Figure 2 can be viewed in color online at [www.glaucomajournal.com](http://www.glaucomajournal.com).

ease of seeing between OCCP and SAP targets at the same decibel level.

On the basis of previous research suggesting that normal thresholds for OCCP reduce with eccentricity,<sup>8</sup> and early model testing, which found more peripheral ODBP targets were seen less frequently than similarly located targets in EVFT, target thresholds were reduced more peripherally to 9 dB, then 8 dB; together with a peripheral magnification factor (Fig. 1B) this mimics the bowl used for the EVFT. Unlike for threshold perimetry commonly used in clinical diagnosis, suprathreshold perimetry thresholds were not age-normalized, as licence requirements are fixed regardless of age. Should the user fail to see a particular locus, then the test is repeated and should the user see a point previously unseen, it is recorded as a false negative (FN). The fixation target (spinning gold star) moves throughout the test to allow for assessment of the full range of the visual field at a comfortable viewing distance, despite limitations of the screen size. The star begins centrally while the blind spot is detected—then it moves to the far left of the screen and the right hemifield is assessed (Fig. 1B); then it moves to the far right of the screen and the left hemifield is assessed.

The following 3 measures are used to ensure the user sits sufficiently close to measure the full binocular field.

- The web application adapts to variances in screen size by adjusting the user's viewing distance and then advising the user at which distance from the monitor to sit—accordingly the user is asked by the application to sit closer for smaller screens and further for larger screens. On average, users typically sit 35–40 cm away from the screen for the OBDP protocol.
- Clearly, not every user will sit at the correct distance. However, the application will locate the user's blind spot, and the OBDP will not proceed unless the blind spot is localized indicating the user is sufficiently close to the monitor to measure the desired field. First, the user is asked by the application, which is their better-seeing eye, and then asked to close their other eye. The test begins thus monocularly, to map the blind spot. To achieve this, small areas were tested on a 4×10 degree



False Positive Rate: 2%  
False Negative Rate: 3%

grid overlying the proposed blind spot, which was estimated at 15 degrees temporal and 0.5 degrees inferior to fixation (Fig. 1E). If the blind spot is detected too far from fixation, users are instructed to move closer to the screen and the process is repeated; similarly if the blind spot is detected too close to fixation the user is asked to move back a little. After detecting the blind spot, the user is asked to open both eyes and the test proceeds binocularly.

- To ensure the user maintains the correct viewing distance during the test, real time webcam monitoring of the head position occurs through the app's facial detection software with a refresh rate of one second. Deviations of facial position monitoring beyond 15% in 4 planes are permitted while those exceeding this threshold were detected, causing the test to pause. Testing would resume once the participant's head position was corrected through verbal instruction.

### OBDP Testing Procedure

Participants initially completed the EVFT and then the OBDP twice, all binocularly. Perimetric testing was undertaken in a dedicated room for the testing on a large-screen (24 inch-diagonal) desktop personal computer (Dell, TX) a resolution of 1920×1080 pixels. The screen was cleaned before testing, and gamma was set at 2.2 and white temperature 6500K. All tests were performed in a standardized way by a trained orthoptist to ensure consistency of protocol. Participants were supervised by a trained orthoptist throughout the test after a briefing on the test expectations and requirements. A sample test printout can be seen in Figure 2. The application is available through the web browser without any downloads required and can be accessed at [www.eyeonic.com](http://www.eyeonic.com).

### Drive Licence Criteria

While guidelines vary for different countries, given the Australian guidelines represent a reasonable consensus point for many different countries, and given this study was performed in Australia, these were chosen as the

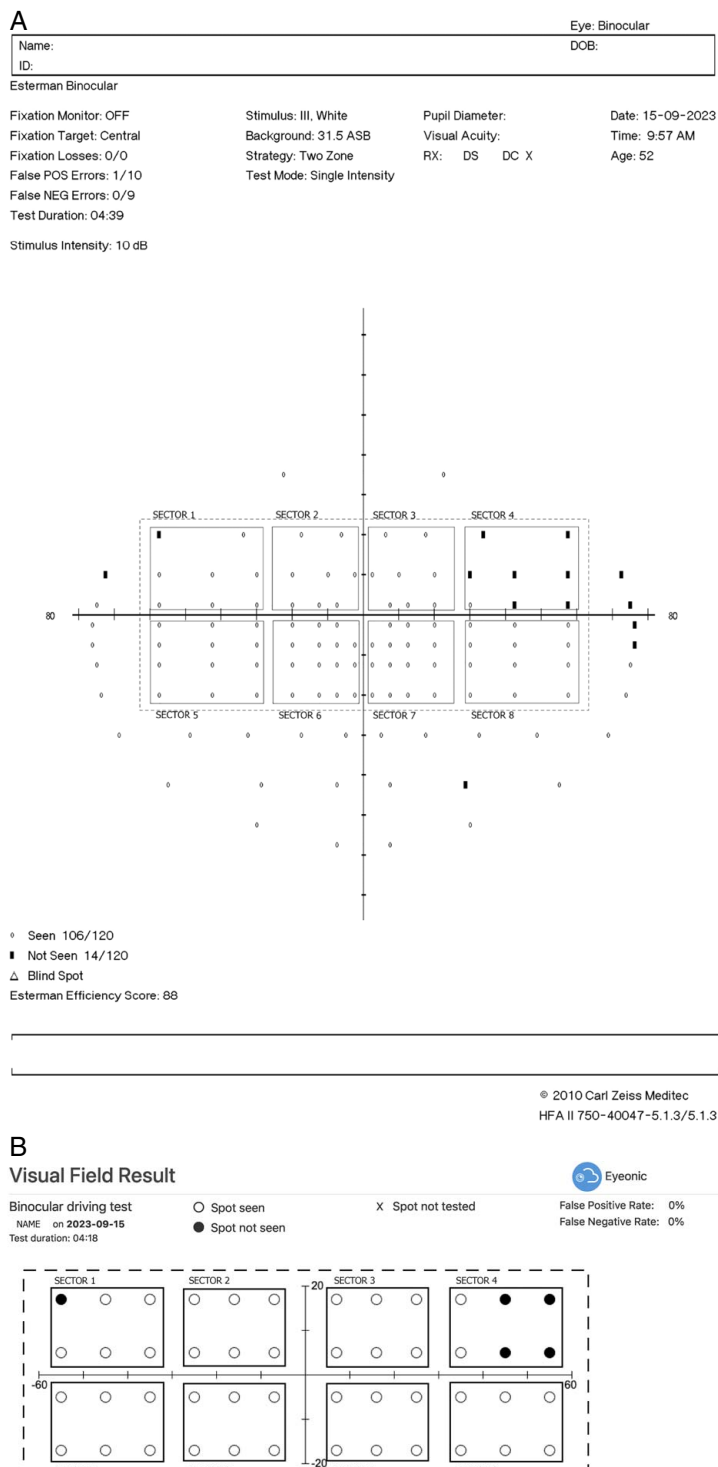


**FIGURE 3.** Division of binocular suprathreshold perimetry tests into 8 sectors for comparative analysis: (A) Esterman visual field test printout, and (B) Online Binocular Driving Perimetry printout from the same participant. This participant had a far upper left point missing in sector 1; and most of the loci missing in the upper right sector 4. Figure 3 can be viewed in color online at [www.glaucousjournal.com](http://www.glaucousjournal.com).

appropriate pass/fail criteria for this study.<sup>41</sup> A horizontal extent of at least 110 degrees within 10 degrees above and below the horizontal midline was required, and a cluster of 4 or more adjoining missed points that is either completely or

partly within the central 20-degree area, or a cluster of 3 adjoining missed points within 20 degrees from fixation, plus any additional separate missed point(s) in the same area, was deemed unacceptable.

**TABLE 1.** Clinical and Perimetric Characteristics

Variables	Control group	Glaucoma group	P
Gender (F/M)	10/8	29/33	0.51
Disease severity			
Mild	—	20	—
Moderate	—	18	—
Severe	—	24	—
Abnormal ONH (%) eyes)	0%	100%	—
Age (y)	60.17 ± 5.00	71.15 ± 3.39	0.002
log MAR visual acuity	-0.02 ± 0.03	0.15 ± 0.05	<0.001
Corrected IOP (mm Hg)	15.00 ± 2.18	13.31 ± 1.28	0.07
CCT (μm)	564.31 ± 15.45	553.19 ± 12.32	0.18
Spherical equivalent (D)	-1.34 ± 1.82	-0.77 ± 0.69	0.44
OCT RNFL			
MT	82.11 ± 6.98	69.80 ± 3.19	<0.001
ST	97.00 ± 10.69	80.04 ± 4.92	0.002
IT	104.08 ± 9.21	75.63 ± 4.82	<0.001
OCT GCC			
MT (μm)	73.81 ± 5.06	63.17 ± 2.61	0.001
ST (μm)	75.25 ± 5.45	63.84 ± 3.61	0.002
IT (μm)	72.17 ± 5.21	60.53 ± 4.45	0.009
SAP			
MD	1.63 ± 0.58	-8.50 ± 1.76	<0.001
PSD	2.09 ± 0.41	6.33 ± 0.93	<0.001
VFI	97.78 ± 1.28	80.15 ± 5.19	<0.001
Normal controls			
% points not seen	EVFT	OBDP	P
Overall	1.42 ± 1.68	0.46 ± 0.45	0.24
Sector 1	4.17 ± 3.69	0.93 ± 1.95	0.08
Sector 2	0.00 ± 0.00	0.00 ± 0.00	—
Sector 3	0.00 ± 0.00	0.00 ± 0.00	—
Sector 4	3.47 ± 4.16	1.85 ± 2.68	0.53
Sector 5	2.31 ± 3.43	0.00 ± 0.00	0.17
Sector 6	0.00 ± 0.00	0.00 ± 0.00	—
Sector 7	0.00 ± 0.00	0.00 ± 0.00	—
Sector 8	2.78 ± 4.02	0.93 ± 1.95	0.41
Test duration (mins:ss)	4:15 ± 0.08	3:04 ± 0:13	<0.001
Duration per point (s)	2.96 ± 0.09	3.83 ± 0.27	<0.001
Glaucoma group			
%Points not seen	EVFT	OBDP	P
Overall	10.9 ± 5.11	9.54 ± 4.73	0.32
Sector 1	17.74 ± 7.40	13.31 ± 7.42	0.12
Sector 2	10.48 ± 6.25	12.23 ± 6.92	0.50
Sector 3	6.65 ± 5.26	6.85 ± 4.63	0.90
Sector 4	15.73 ± 6.80	12.77 ± 5.60	0.26
Sector 5	14.52 ± 7.56	12.10 ± 6.69	0.29
Sector 6	7.31 ± 5.22	7.26 ± 5.75	0.97
Sector 7	5.81 ± 3.86	5.11 ± 4.02	0.65
Sector 8	11.83 ± 6.32	6.99 ± 4.52	0.05
Test duration (mins:ss)	4:37 ± 0:14	3:02 ± 0:09	<0.001
Duration per point tested (s)	3.59 ± 0.20	4.57 ± 0.43	<0.001

Values are presented as mean ± 95% CI unless otherwise specified.

CCT indicates central corneal thickness; D, diopters; EVFT, Esterman visual field testing; GCC, ganglion cell complex inner plexiform layer; IOP, intraocular pressure; IT, inferior thickness; MAR, minimal angle of resolution; MD, mean deviation; MT, mean thickness; OCBDP, online computer-based binocular driving perimetry assessment; OCT, optical coherence tomography; ONH, optic nerve head; PSD, pattern standard deviation; RNFL, retinal nerve fiber layer; SAP, standard automated perimetry; ST, superior thickness; VFI, visual field index.

## Statistical Analysis

Statistical analysis was performed using the Statistical Package for Social Sciences<sup>38</sup> and Real Statistics in Excel 2016 (Microsoft 365). A significance level of  $P < 0.05$  was applied with adjustment by the Bonferroni method. Normality of data was evaluated with the Shapiro-Wilk statistic. Comparisons between baseline data of normal controls and glaucomatous eyes were made using either the independent  $t$  test for normally distributed data or the Mann-Whitney  $U$  test for nonparametric data.

To assess for regional agreement between the OBDP and EVFT, the binocular field was subdivided into 8 sectors (Fig. 3). For comparison between EVFT and OBDP, the first OBDP test was used.

The main outcome measures were:

The percentage ratio of points not seen (%PNS) to points presented, calculated individually for each sector (1–8), and for the whole 120 by 40 degree field, for both the OBDP and the central 120 by 40 degrees of the EVFT.

The number of contiguous points not seen in the central 20 degrees of the OBDP, used to calculate sensitivity and specificity compared with the EVFT and HFA 24-2 using current Australian licensing criteria.

The repeatability of the OBDP, overall and per sector.

Bland-Altman analyses were used to analyse the agreement and estimate the 95% limits of agreement (LoA) for the %PNS per sector and per 120 by 40 degree field. Correlation between EVFT and OBDP was assessed using intraclass coefficients (ICCs) and simple linear regression analyses with Pearson coefficient, while ICCs were used to assess OBDP test-retest repeatability. ICCs were defined as excellent ( $\geq 0.9$ ); good (0.75–0.9); moderate (0.5–0.75); or poor ( $< 0.5$ ).<sup>39</sup> Pearson values were defined as strong ( $> 0.75$ ); moderate (0.45–0.75); weak (0.25–0.45) or very weak ( $< 0.25$ ).<sup>40</sup>

To assess the diagnostic accuracy of the OBDP, sensitivity and specificity values were calculated against both the EVFT and the HFA 24-2 (IVF) using pass/fail criteria adapted from the Austroads guidelines for private driver licensing.<sup>41</sup>

## RESULTS

Table 1 represents the baseline demographic characteristics of the 80 participants enrolled in the study, with a mean age of 68.68 ( $\pm 2.99$ ) years. Of these, 49% were female; 18 were healthy controls, while 20, 18, and 24 had mild, moderate and severe glaucoma, respectively. The overall mean testing time for OBDP (48 loci tested) was significantly shorter than EVFT (86 loci tested) in both the glaucoma (3:02 ± 0:09 vs. 4:37 ± 0:14,  $P < 0.001$ ) and control group (3:04 ± 0:13 vs. 4:15 ± 0:08,  $P < 0.001$ ). However, mean testing time per locus was significantly shorter for EVFT than OBDP in both groups ( $P < 0.001$ ). When EVFT and OBDP tests were compared, there were no significant differences observed in %PNS for both glaucoma (10.9 ± 5.11 vs. 9.54 ± 4.73,  $P = 0.32$ ) and control groups (1.42 ± 1.68 vs. 0.46 ± 0.45,  $P = 0.24$ ) overall, and for each sector except Sector 8 in the glaucoma group ( $P = 0.05$ ).

Figure 4 displays the reliability indices for EVFT compared with OBDP. Figure 4A displays results for the control group, while Figure 4B involves participants with glaucoma. For both groups, no statistically significant changes were observed between the EVFT and OBDP FP rates. However, FN rates were significantly lower for EVFT

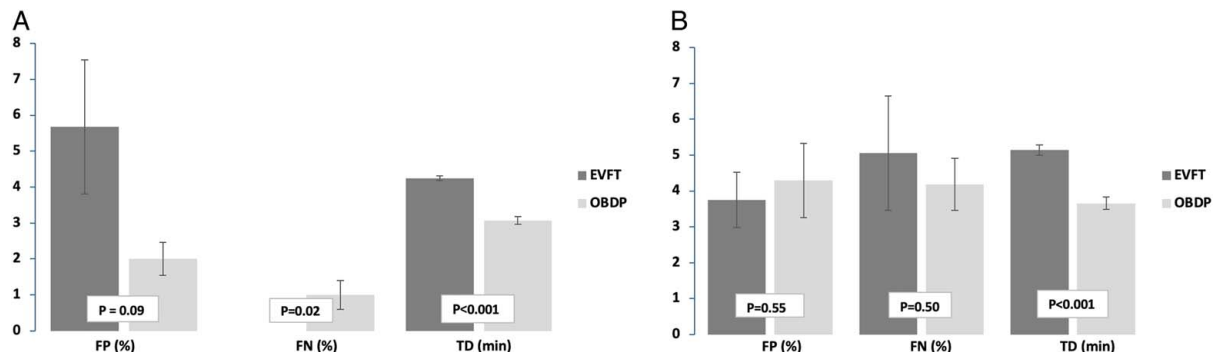


**FIGURE 4.** A comparison of EVFT and OBDP testing reliability indices and test time. (A) Control group. (B) Glaucoma group. FP indicates false positive; FN, false negative; TD, test duration. Error bars indicate standard error (SE). Figure 4 can be viewed in color online at [www.glaucosjournal.com](http://www.glaucosjournal.com).

testing compared with OBDP in the control group ( $P=0.02$ ).

### Comparison of OBDP to EVFT

Table 2 presents Pearson correlation coefficients, intraclass coefficients, Bland Altman bias and corresponding limits of agreement for the %PNS for all 8 sectors combined and per sector when comparing OBDP and EVFT testing results. ICCs evaluating the agreement of % PNS ranged from good to excellent (0.76–0.93) when individual sectors of the binocular field were compared, and excellent (0.93) for the overall visual field.

Figure 5 displays Bland Altman Plots and linear regression correlation curves for the %PNS corresponding to each sector when EVFT and OBDP results were compared. Testing Bias ranged from  $-1.35\%$  for sector 2 (LoA:  $-36.65\%$  to  $33.94\%$ ) to  $4.17\%$  for sector 8 (LoA:  $-29.62\%$  to  $37.95\%$ ), with sector 6 demonstrating the smallest bias between the 2 tests at  $0.04\%$  (LoA:  $-18.96\%$  to  $19.05\%$ ). In general, LoA were wider for more peripheral sectors (1, 4, 5, and 8) than central sectors (2, 3, 6, and 7). Pearson correlation coefficients ranged from moderate to strong per sector (0.65–0.88), with the smallest and largest values demonstrated by sectors 8 and 6, respectively.

Figure 6A displays the Bland Altman plot for %PNS for the entire 120 by 40 degree field when OBDP and EVFT tests were compared, with a test bias of  $1.24\%$  (LoA:  $-16.83\%$  to  $19.30\%$ ). Figure 6B presents the corresponding linear regression curve, with a correlation coefficient of  $0.86$  ( $P<0.001$ ).

Sensitivities of the OBDP were evaluated using criteria adapted from the Austroads driving guidelines as outlined

above. When compared with the EVFT, the OBDP demonstrated a sensitivity of 96.97%, specificity of 78.57%, and a positive predictive value (PPV) of 95.52%. With respect to the HFA 24-2 (IVF), the OBDP showed a sensitivity of 98.41%, specificity of 58.82%, and PPV of 89.86%. Lastly, when the EVFT was compared directly to the HFA 24-2 (IVF), there was a sensitivity of 92.06%, specificity of 52.9% and a PPV of 87.88%.

### Repeatability of OBDP

Table 3 presents the repeatability of the OBDP using intraclass coefficients for the whole field, and for each of the 8 sectors individually. ICCs evaluating the repeatability of OBDP testing for percentage of points not seen were excellent overall (0.97) and ranged from moderate to excellent for each of the 8 sectors (0.67–0.98).

Figure 6C displays the Bland Altman Plot for the %PNS for the entire 120 by 40 degree field when the 2 repeat OBDP tests were compared, with a test bias of  $-0.36\%$  (LoA:  $-14.75\%$  to  $14.02\%$ ).

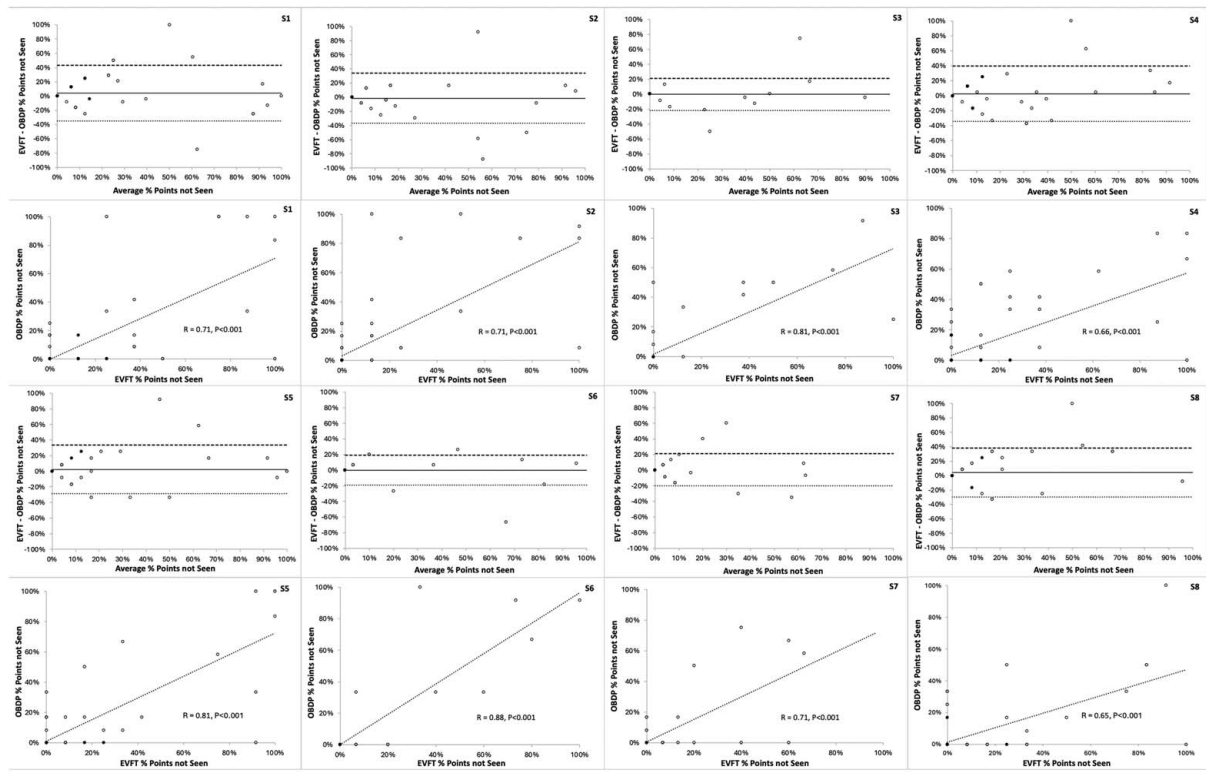
Figure 7 shows Bland Altman Plots for the %PNS corresponding to each sector when the 2 repeat OBDP tests were compared. Testing bias ranged from  $-2.59\%$  for sector 1 (LoA:  $-32.10\%$  to  $26.92\%$ ) to  $1.14\%$  for sector 2 (LoA:  $-16.68\%$  to  $18.96\%$ ). A bias of  $0.00\%$  was observed for both sector 5 (LoA:  $-19.93\%$  to  $19.93\%$ ) and sector 7 ( $-22.28\%$  to  $22.28\%$ ).

Figure 8 shows a selection of Esterman visual fields, alongside the respective patient's online binocular perimetry visual field test, for illustrative purposes.

**TABLE 2.** Comparison of Points Not Seen on EVFT and OBDP

EVFT vs. OBDP	Pearson correlation coefficient	ICC (95% CI)	Bland Altman bias (%)	Bland Altman 95% LoA (%)
Overall %PNS	$R = 0.86, P < 0.001$	$0.93 (0.88–0.95)$	$1.24$	$(-16.83 \text{ to } 19.30)$
Sector 1%PNS	$R = 0.71, P < 0.001$	$0.83 (0.74–0.89)$	$4.17$	$(-34.90 \text{ to } 43.24)$
Sector 2%PNS	$R = 0.71, P < 0.001$	$0.83 (0.73–0.89)$	$-1.35$	$(-36.65 \text{ to } 33.94)$
Sector 3%PNS	$R = 0.81, P < 0.001$	$0.89 (0.83–0.93)$	$-0.16$	$(-21.68 \text{ to } 21.37)$
Sector 4%PNS	$R = 0.66, P < 0.001$	$0.79 (0.66–0.86)$	$2.66$	$(-34.22 \text{ to } 39.53)$
Sector 5%PNS	$R = 0.81, P < 0.001$	$0.89 (0.83–0.93)$	$2.40$	$(-28.70 \text{ to } 33.49)$
Sector 6%PNS	$R = 0.88, P < 0.001$	$0.93 (0.89–0.96)$	$0.04$	$(-18.96 \text{ to } 19.05)$
Sector 7%PNS	$R = 0.71, P < 0.001$	$0.83 (0.73–0.89)$	$0.54$	$(-20.23 \text{ to } 21.32)$
Sector 8%PNS	$R = 0.65, P < 0.001$	$0.76 (0.62–0.85)$	$4.17$	$(-29.62 \text{ to } 37.95)$

%PNS indicates percentage ratio of Points not Seen/Points presented; ICC, intraclass correlation coefficient; LoA, 95% limits of agreement.



**FIGURE 5.** Bland Altman Plots and linear regression curves for the percentage of points not seen corresponding to each sector (S1–S8) when EVFT and OBDP results were compared. The continuous and dotted horizontal lines represent the mean difference (bias) and 95% limits of agreement (Bias  $\pm$  1.96SD). Black-colored circles represent controls and white-colored circles represent glaucomatous eyes, with overlap of individual points permitted.

## DISCUSSION

OBDP was successfully utilized as an online binocular wide field licence assessment in a cohort of 62 patients with mild, moderate, or severe glaucoma and 18 controls. It has moderate to strong agreement and correlation with EVFT utilizing Bland Altman plots, ICC and Pearson correlation. Repeatability of the OBDP was moderate to excellent. When compared with both the Esterman and binocularly integrated HFA 24-2 tests using Australian driving guidelines, sensitivities ranged from 96% to 98%, indicating an excellent level of agreement with both tests. Specificity was lower, at 79% compared with EVFT, and 59% compared

with 24-2 IVF; however, the EVFT had an even lower specificity compared with EVFT (52%) indicating a potential problematic relationship between binocular 24-2 IVF and binocular suprathreshold perimetry. The agreement, correlation, and repeatability of testing parameters between both groups is consistent with previous studies comparing OCCP and SAP for 24-2 threshold perimetry.<sup>8,16,17,20</sup>

The overall comparison of OBDP and EVFT tests displayed limits of agreement (LoA) of  $-16.83$  to  $19.30$  percentage points (with a test vials of 1.24%). A study looking at the same-day repeatability of EVFT tests showed

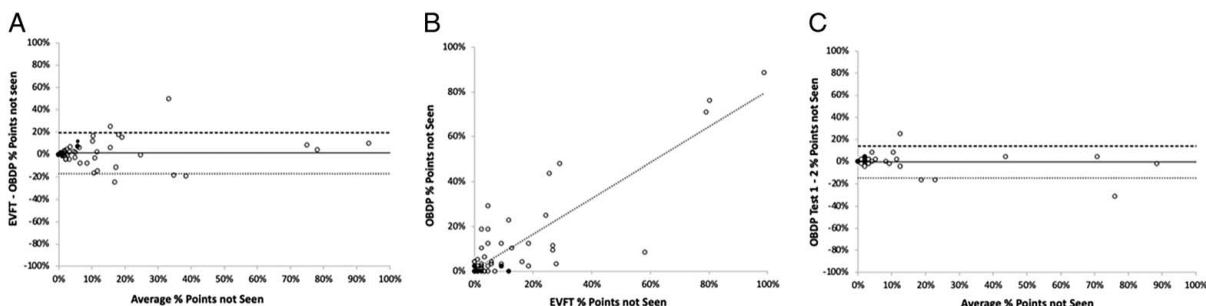


**FIGURE 6.** (A) Bland Altman Plot for the overall percentage of points not seen (%PNS) when OBDP and EVFT tests were compared. (B) Linear regression curve for the overall %PNS when OBDP and EVFT tests were compared. (C) Bland Altman Plot for the overall %PNS when the 2 repeat OBDP tests were compared. Continuous and dotted horizontal lines represent the mean difference (bias) and 95% limits of agreement (Bias  $\pm$  1.96SD). Black-colored circles represent controls and white-colored circles represent glaucomatous eyes, with overlap of individual points permitted.

**TABLE 3.** Comparison of Intraclass Coefficients for OBDP Tests 1 and 2

OBDP test 1 vs. OBDP test 2	ICC (95% CI)
Whole field %PNS	0.97 (0.94–0.98)
Sector 1%PNS	0.93 (0.87–0.96)
Sector 2%PNS	0.97 (0.95–0.98)
Sector 3%PNS	0.91 (0.84–0.95)
Sector 4%PNS	0.76 (0.56–0.87)
Sector 5%PNS	0.96 (0.93–0.98)
Sector 6%PNS	0.98 (0.97–0.99)
Sector 7%PNS	0.89 (0.80–0.94)
Sector 8%PNS	0.67 (0.39–0.82)

%PNS indicates percentage ratio of points not seen/points presented; ICC, intraclass correlation coefficient.

LoA of  $-8.96$  and  $9.45$ , and showed peripheral test points to be less reliable than central points.<sup>41</sup> Therefore, a degree of variability in results undertaken on the same device is expected, and as such, given the other fundamental perimetric differences between OBDP and EFVT, the comparison between the technologies shows promise for further development and evaluation.<sup>42</sup>

The overall LoA for OBDP repeatability was  $-14.75\%$  to  $14.02\%$ . Given EFVT was not repeated in this study, the LoA of repeatability for EFVT can be best estimated from Fujimoto et al,<sup>41</sup> indicating a stronger repeatability of EFVT over OBDP. Such a comparison to unmatched data must be performed with caution, and future studies can directly compare the repeatability of the 2 suprathreshold binocular perimetry methods.

These results suggest the OBDP can potentially be used in the detection of visual field defects that could limit driving and that OBDP holds promise as a driving assessment screening tool in both normal subjects and those with mild, moderate, and severe glaucoma. While it may complement existing clinic perimetry, the goal is to provide a cost-effective solution within and outside of traditional clinics, especially for remote and rural communities with limited access to conventional perimetry machines. This may help providers utilize a simple and cost-effective screening tool to

determine if a patient requires further, more standardized testing of their driving performance and fitness to drive. The browser-based web platform and minimal hardware requirements make OBDP a widely accessible and cost-effective test.

While other OCCP protocols (10-2, 24-2, and 30-2) can be performed on any tablet or computer, given the wider screen requirements the OBDP protocol is restricted to computers only; that is, the app will not allow the OBDP protocol for use on tablets.

The advantage of OBDP is that it operates on any computer, without additional software or hardware, has minimal processing requirements and is easy to use.<sup>16</sup> This has significant benefits in terms of access and affordability for patients and health funders alike, as well as usability and space conservation in a clinic. The ability of this test to be performed on a familiar device reduces anxiety for patients and potential adverse effects, such as poor adherence and test performance.<sup>43</sup> The OBDP allows for easy comparison between test results and requires little interpretation.

All subjects in this cohort were closely supervised by a trained orthoptist. To allow for licence screening for unsupervised remote or at home scenarios, certain modifications would be beneficial, including gaze tracking and facial recognition in complement to facial detection to ensure the correct person is indeed performing the test. In addition, the test needs to be evaluated with induced variability, such as in different rooms, with different monitors, and different ambient lighting conditions. Future studies will evaluate the accuracy of OCCP testing with these variations and in an unsupervised home environment. Ongoing improvements of the application delivering OBDP will provide better instructions to patients to provide the level of education given by the supervising orthoptist in this study.

Other studies have evaluated perimetry delivered on various devices.<sup>1,3,4,9,10,44</sup> Computer, tablet, and mobile-based achromatic perimetry has been previously reported to discriminate between control and glaucomatous eyes and correlate well with standard automated perimetry in a clinical setting. However, to date, only one study by

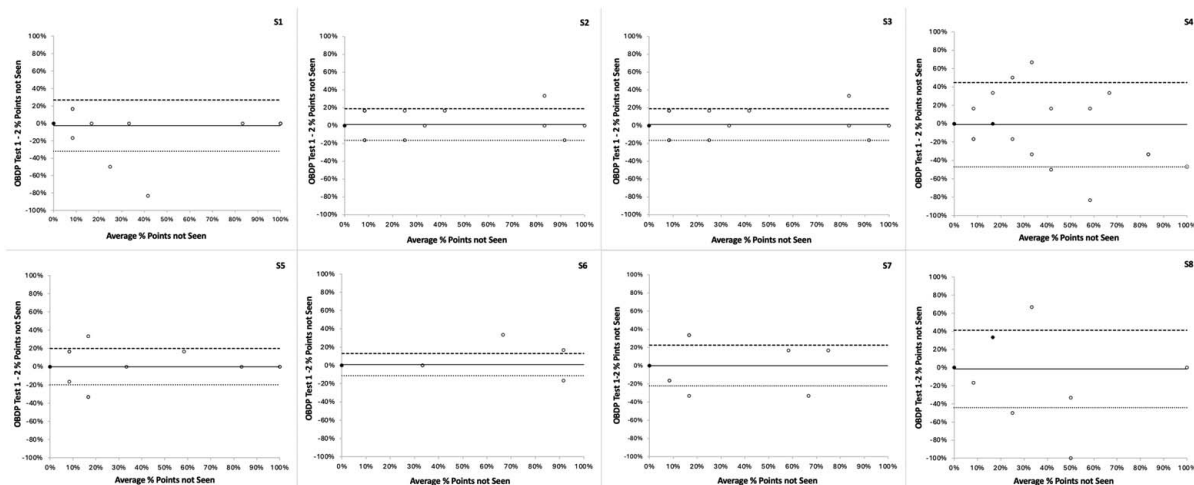


**FIGURE 7.** Bland Altman Plots for the percentage of points not seen corresponding to each sector (S1–S8) when the 2 repeat OBDP tests were compared. Black-colored circles represent controls and white-colored circles represent glaucomatous eyes, with overlap of individual points permitted.

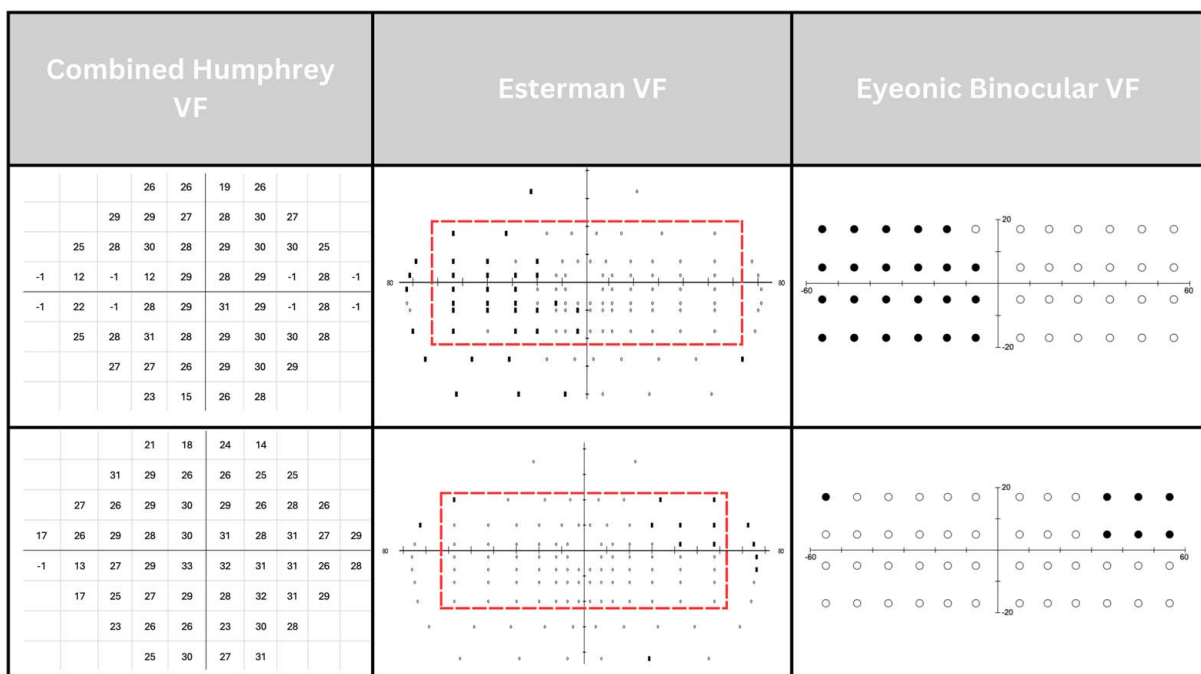


**FIGURE 8.** (A, B). Assorted visual comparison of EVFT with OBDP for the corresponding patient. EVFT dashed-box indicates area included in OBDP test. Figure 8 can be viewed in color online at [www.glaucousjournal.com](http://www.glaucousjournal.com).

Sharma et al<sup>45</sup> has evaluated a driving assessment protocol on a portable perimetry device, namely a virtual reality visual field headset (VRVF). Compared with the OBDP, Sharma and colleagues study found “concordance between VRVF and (Standard Automated Perimetry, SAP) test using point-by-point analysis was poor” and that “based on the weak overall agreement between VRVF and SAP, the current VRVF EVFT is not an acceptable determinant of driver’s licensing.” In comparison, the metrics in the current paper are sufficient to consider further evaluation of the use of OBDP as a screening tool for consideration of standardized driving assessment using the EVFT. While binocular perimetry is a widely accepted modality for assessing visual fitness to drive, the specific requirements and interpretation of results are not internationally standardized and can vary substantially between different jurisdictions.<sup>12,13</sup> Therefore, a thorough understanding of the prevailing local guidelines is essential for clinicians. There are concerns, for example, that the Esterman program may not accurately capture central visual field loss relevant to European driving standards, highlighting the need for a more standardized approach.<sup>13,46</sup>

In this study, the monitor used was at a predetermined size, resolution, and brightness level. Standardized environmental testing conditions were also maintained. Patients were closely monitored by trained staff to ensure optimal positioning and use of the web-based application. One concern logically about web-based perimetry is the inconsistencies in screen size and luminance between different computer monitors, which could impact test reliability.<sup>47</sup> However, the application has many inbuilt features to ensure consistency of display. These range from the type, size, flicker rate of the targets, the screen background, internal calibration based on initial responses, and the app requiring the user to manually increase screen brightness to

at least 75%. While all of these mechanisms are designed to achieve consistency despite variations in differences in screen capacities and home lighting environments, further research on tests undertaken in unregulated environments will be useful. All perimetry devices record increased variability at damaged loci with low sensitivity compared with normal sensitivity loci; however, the gamma relationship inherent in web-based perimetry can become harder to characterize for extreme cases (eg, points with  $rgb < 0,0,0 >$  dark minima, corresponding to 0 rdB). The impact of interscreen inconsistencies needs to be considered in the context of the advantage of web-based, device-agnostic perimetry in terms of scalability, accessibility, and affordability.

The positioning of the test loci is automatically adjusted based on the screen size to achieve consistency in viewing angle, and this is determined at the test outset, with the web-based application automatically detecting monitor size and thereby optimizing viewing distance. In addition to blind spot localization, this positions the test targets accordingly. Head positioning and posture can be maintained using the combination of predetermined the appropriate viewing distance, blind spot localization, and AI-face monitoring.<sup>15</sup> While each of these mechanisms has its own error rate, given their independence, when used together there is a calculated error rate of < 1%.<sup>48</sup> While consistency of viewing distance is achieved in other devices using a chin rest or hood, the advantage of the OBDP technology works best without any additional hardware requirements. In addition, clear instructions (in multilingual options) are provided to patients at the initiation of the test, which are important to maintain posture and positioning.

One critical aspect of licence assessment is the motivation of individuals to cheat, which was not present for the participants of this study. The most critical way that

individuals might try to cheat the test is by fixation movements. With the current system, when the fixation target is on the right of the screen, the subject knows which hemifield is being assessed; so they can shift their fixation further left, increasing their probability of seeing the stimulus and hence increasing their probability of keeping their driving license. This problem does not occur for the standard EVFT, since stimuli can appear on either side of the fixation target. In addition, unsupervised individuals might cheat by substituting another person to perform the test in their place. Thankfully, both of these issues can be addressed by expanding the role of artificial intelligence, specifically computer vision. The use of gaze-tracking would allow for measurement of fixation loss and prevent deceptive movement by patients who are aware of their hemifield defect. Facial recognition would also confirm the identification of the person completing the test. These aspects are currently in development for addition to the OBDP soon.

Motivation to pass the test could also result in excessive clicking of the mouse. To counter this a strict system of FPs based on a tailored interstimulus range and catch trials, as well as a negative sound when a mis-timed click is performed, and a random addition to the interstimulus interval are inbuilt into the design. A strict cutoff for FP can be introduced for passing a licence test.

Increased test variability was noted for more peripheral than central points. This is true for both OBDP and EVFT.<sup>41</sup> There could be several reasons for this. First, the issue of gaze wandering across the screen, which might magnify the difference between OBDP and EVFT, is greater for more peripheral than central stimuli. Second, the discrepancy between the flat screen and bowl is greater for peripheral than central stimuli. Third, the 3 complementary mechanisms of maintenance of viewing distance, described above, might lead to more errors in peripheral than central sampling. A solution for the first problem is discussed above with AI gaze tracking; for the second problem, the data from this study can be used to further modify the peripheral threshold correction and magnification factor. For the third problem, a tighter allowance of head movement deviation may be required (eg, reducing the trigger to ask the patient to reposition from 15% to 10% of deviation in face monitoring).

Limits of agreement on Bland Altman plots often exceeded  $\pm 20\%$  when EVFT and OBDP were compared. This degree of test variability aligns with findings from other studies evaluating portable perimetric devices and may be expected with the shift to more flexible, screen-based testing methods.<sup>44</sup> For example, Kumar and Thulasidas (2020) reported limits of agreement of approximately  $\pm 6$  dB in mean deviation when comparing a novel tablet perimeter to SAP.<sup>47</sup> Moreover, higher test variability should be considered alongside other significant advantages of digital perimetry, including greater test accessibility and the potential for more frequent testing.<sup>48–50</sup> Further planned advancements in OBDP software, as discussed earlier, may also help enhance future testing accuracy for licensing purposes.

Other limitations of the study include the collection of patients from a single ophthalmology practice, with the potential to introduce selection bias. Given the incidence of glaucoma in the cohort, patients with other visually limiting pathology, such as retinal diseases, were intentionally excluded in order to prioritize consistency in our results. Further studies on larger cohorts would be useful to assess

the use of OBDP in non-glaucomatous visual pathology. Patients performed repeated OBDP shortly after the EVFT, which might have performance implications, such as concentration and fatigue. Randomized order of testing would be ideal, and should be considered in future studies, but was not possible in the current study given the constraints of patient enrollment from a busy clinical practice. While the OBDP adjusts patient viewing distance with blind spot mapping, data was not collected on the frequency of patient drift or the number of adjustments required. Anecdotally, this occurred on average once per every 2 tests; however, further data could be collected in future studies for objective quantification. The reliability parameters utilized were similar to those obtained from the EVFT, and correlation was predominantly sought from missing data points between the 2 tests rather than the reliability of detecting all points.

## CONCLUSIONS

OBDP showed strong agreement with EVFT. As an online application that easily runs on any computer, it has the potential to expand the scope of binocular perimetry screening for future development of standardized, regulation-compliant online perimetry tools. Further modifications are required to make the protocol suitable for at home licencing assessment. With such modifications integration into routine clinical practice could be considered.

## REFERENCES

1. Prea SM, Kong DYX, Guymer RH, et al. Uptake, persistence, and performance of weekly home monitoring of visual field in a large cohort of patients with glaucoma. *Am J Ophthalmol*. 2021; 223:286–295.
2. Lowry EA, Hou J, Hennein L, et al. Comparison of peristaltic online perimetry with the Humphrey perimetry in a clinic-based setting. *Transl Vis Sci Technol*. 2016;5:4.
3. Schulz AM, Graham EC, You Y, et al. Performance of iPad-based threshold perimetry in glaucoma and controls. *Clin Exp Ophthalmol*. 2018;46:346–355.
4. Kong YX, He M, Crowston JG, et al. A comparison of perimetric results from a tablet perimeter and Humphrey field analyzer in glaucoma patients. *Transl Vis Sci Technol*. 2016;5:2.
5. Alawa KA, Nolan RP, Han E, et al. Low-cost, smartphone-based frequency doubling technology visual field testing using a head-mounted display. *Br J Ophthalmol*. 2021;105:440–444.
6. Tsapakis S, Papaconstantinou D, Diagouras A, et al. Visual field examination method using virtual reality glasses compared with the Humphrey perimeter. *Clin Ophthalmol*. 2017;11: 1431–1443.
7. Deiner MS, Damato BE, Ou Y. Implementing and monitoring at-home virtual reality oculo-kinetic perimetry during COVID-19. *Ophthalmol*. 2020;127:1258.
8. Skalicky SE, Bigirimana D, Busija L. Online circular contrast perimetry via a web-application: optimising parameters and establishing a normative database. *Eye*. 2023;37:1184–90.
9. Jones PR, Smith ND, Bi W, et al. Portable perimetry using eye-tracking on a tablet computer - a feasibility assessment. *Transl Vis Sci Technol*. 2019;8:17.
10. Aboobakar IF, Friedman DS. Home monitoring of glaucoma: current applications and future directions. *Semin Ophthalmol*. 2021;36:310–314.
11. Austroads. Assessing Fitness to Drive 2022, Austroads Ltd, Sydney NSW, 2022. [https://austroads.com.au/\\_data/assets/pdf\\_file/0037/498691/AP-G56-22\\_Assessing\\_Fitness\\_Drive.pdf](https://austroads.com.au/_data/assets/pdf_file/0037/498691/AP-G56-22_Assessing_Fitness_Drive.pdf)
12. Yan MK, Kumar H, Kerr N, et al. Transnational review of visual standards for driving: How Australia compares with the rest of the world. *Clin Exp Ophthalmol*. 2019;47:847–863.

13. Sudmann TM, Jonsdottir TE, Rowe FJ, et al. National application of the European visual field standards for driving: a survey study. *BMJ Open Ophthalmol*. 2022;7:e000904.
14. Ruia S, Tripathy K. *Humphrey Visual Field*. StatPearls Publishing; 2023.
15. Chen YX, Meyerov J, Skalicky SE. Online circular contrast perimetry via web-application: establishing a normative database for central 10-degree perimetry. *Clin Ophthalmol*. 2024;18: 201–13.
16. Meyerov J, Deng Y, Busija L, et al. Circular contrast perimetry via web application: a patient appraisal and comparison to standard automated perimetry. *Ophthalmol Sci*. 2022;2:100172.
17. Hoang TT, Mai TQ, Pham DT, et al. Glaucoma clinic monitoring over 6 months using online circular contrast perimetry in comparison with standard automatic perimetry: the developing-world setting. *clinical Ophthalmology*. 2024;14: 3767–3780.
18. Meyerov J, Deng Y, Busija L, et al. Online circular contrast perimetry: a comparison to standard automated perimetry. *Asia-Pacific J Ophthalmol*. 2023;12:4–15.
19. Tan JCK, Yohannan J, Ramulu PY, et al. Visual field testing in glaucoma using the swedish interactive thresholding algorithm (SITA). *Surv Ophthalmol*. 2025;70:141–152.
20. Meyerov J, Chen YX, Busija L, et al. Repeatability of online circular contrast perimetry compared to standard automated perimetry. *J Glaucoma*. 2024;33:505–515.
21. Chylack LT Jr, Wolfe JK, Singer DM. The lens opacities classification system III. The longitudinal study of cataract study group. *Arch Ophthalmol*. 1993;111:836.
22. Gedde SJ, Vinod K, Wright MM, et al. Primary open-angle glaucoma preferred practice pattern. *Ophthalmology*. 2021;128: 71–150.
23. Callan Thomas. *Humphrey Instruments*. Dublin, CA, USA: Zeiss Group Global, 2023.
24. Ishibashi M, Matsumoto C, Hashimoto S, et al. Utility of CLOCK CHART binocular edition for self-checking the binocular visual field in patients with glaucoma. *Br J Ophthalmol*. 2019;103:1672–1676.
25. Zeppieri M, Brusini P, Parisi L, et al. Pulsar perimetry in the diagnosis of early glaucoma. *Am J Ophthalmol*. 2010;149: 102–112.
26. González-Hernández M, García-Feijoó J, Sanchez Mendez M, et al. Combined spatial, contrast, and temporal functions perimetry in mild glaucoma and ocular hypertension. *Eur J Ophthalmol*. 2004;14:514–522.
27. Anderson AJ, Johnson CA, Ginferet M, et al. Characteristics of the normative database for the Humphrey matrix perimeter. *Invest Ophthalmol Vis Sci*. 2005;46:1540–1548.
28. Swanson WH, Horner DG, Dul MW, et al. Choice of stimulus range and size can reduce test-retest variability in glaucomatous visual field defects. *Transl Vis Sci Technol*. 2014;3:6.
29. Liu S, Yu M, Lai G, et al. Frequency-doubling technology perimetry for detection of the development of visual field defects in glaucoma suspect eyes: a prospective study. *JAMA Ophthalmol*. 2014;132:77–83.
30. Johnson CA, Cioffi GA, Van Buskirk EM. Frequency doubling technology perimetry using a 24-2 stimulus presentation pattern. *Optom Vis Sci*. 1999;76:571–581.
31. Warren DE, Thurtell MJ, Carroll JN, et al. Perimetric evaluation of saccadic latency, saccadic accuracy, and visual threshold for peripheral visual stimuli in young compared with older adults. *Invest Ophthalmol Vis Sci*. 2013;54:5778–5787.
32. Anderson AJ, Vingrys AJ. Interactions between flicker thresholds and luminance pedestals. *Vision Res*. 2000;40:2579–2588.
33. WCAG WG. Relative Luminance. Accessed April 22, 2024. [https://www.w3.org/WAI/GL/wiki/Relative\\_Luminance](https://www.w3.org/WAI/GL/wiki/Relative_Luminance); 2021.
34. Campbell FW, Green DG. Optical and retinal factors affecting visual resolution. *J Physiol*. 1965;181:576–593.
35. Mulholland PJ, Garway-Heath DF, Anderson RS, et al. Spatiotemporal summation of perimetric stimuli in early glaucoma. *Invest Ophthalmol Vis Sci*. 2015;56:6473–6482.
36. Pan F, Swanson WH, Dul MW. Evaluation of a two-stage neural model of glaucomatous defect: an approach to reduce test-retest variability. *Optom Vis Sci*. 2006;83:499–511.
37. Anderson RS, Redmond T, McDowell DR, et al. The robustness of various forms of perimetry to different levels of induced intraocular stray light. *Invest Ophthalmol Vis Sci*. 2009;50:4022–4028.
38. SPSS, Inc., Chicago, IL, USA. IBM.
39. Koo TK, Li MY. A guideline of selecting and reporting intraclass correlation coefficients for reliability research. *J Chiropr Med*. 2016;15:155–163.
40. Akoglu H. User's guide to correlation coefficients. *Turk J Emerg Med*. 2018;18:91–93.
41. Fujimoto S, Ikesugi K, Ichio T, et al. Reliability of binocular Esterman visual field test in patients with glaucoma and other ocular conditions. *Diagnostics*. 2024;14:433.
42. Kaliaperumal S, Janani VS, Menon V, et al. Study of anxiety in patients with glaucoma undergoing standard automated perimetry and optical coherence tomography—a prospective comparative study. *Indian J Ophthalmol*. 2022;70:2883–2887.
43. Huang OS, Chew ACY, Finkelstein EA, et al. Outcomes of an asynchronous virtual glaucoma clinic in monitoring patients at low risk of glaucoma progression. *Asia Pac J Ophthalmol*. 2021;10:328–334.
44. Jones PR, Campbell P, Callaghan T, et al. Glaucoma home monitoring using a tablet-based visual field test (eyecatcher): an assessment of accuracy and adherence over 6 months. *Am J Ophthalmol*. 2021;223:42–52.
45. Sharma M, Savatovsky E, Huertas L, et al. Esterman visual field testing using a virtual reality headset in glaucoma. *Ophthalmol Sci*. 2024;4:100534.
46. Innerdal C, Ekstrand JR, Wankel VD, et al. Visual field requirements for driving in Europe: the risk of inaccurate interpretation of visual field findings when using the binocular Esterman programme. *Acta Ophthalmol*. 2019;97:e939–e941.
47. Tahir HJ, Murray IJ, Parry NR, et al. Optimisation and assessment of three modern touch screen tablet computers for clinical vision testing. *PLoS ONE*. 2014;9:e95074.
48. External data: Australian Therapeutics Goods Association Software Engineering department 2024.
49. Kumar H, Thulasidas M. Comparison of perimetric outcomes from Melbourne Rapid Fields tablet perimeter software and Humphry Field Analyzer in glaucoma patients. *J Ophthalmol*. 2020;8384509.
50. Chia ZK, Kong AW, Turner ML, et al. Assessment of remote training, at-home testing, and test-retest variability of a novel test for clustered virtual reality perimetry. *Ophthalmol Glau*. 2023;7:139–147.